Floquet SPT-MBL in a 6-Qubit System

Shiva Heidari[1]

[1]Theoretical Condensed Matter Physicist

1 Introduction

Periodically driven quantum systems, commonly referred to as *Floquet systems* [1], offer a powerful framework for exploring exotic phases of matter far from equilibrium [2]. Unlike equilibrium phases, which are governed by ground-state properties of time-independent Hamiltonians, Floquet phases emerge in systems with explicit time-periodicity in the Hamiltonian. That is, the dynamics are governed by a Hamiltonian satisfying

$$H(t+T) = H(t),$$

where T is the driving period. This temporal periodicity allows one to define the evolution over a single period using the *Floquet unitary operator*[3, 1, 4]:

$$U_F = \mathcal{T} \exp\left(-i \int_0^T H(t)\, dt\right),$$

where $\mathcal{T}$ denotes time ordering. The eigenstates of U_F, denoted by $|\phi_\alpha\rangle$, are called *Floquet eigenstates*, and their associated eigenvalues take the form $e^{-i\varepsilon_\alpha T}$, where $\varepsilon_\alpha \in [-\pi/T, \pi/T)$ are known as *quasienergies*. Since quasienergies are defined modulo $2\pi/T$, the Floquet spectrum forms a compact Brillouin zone analogous to momentum in crystalline solids.

A key question in the study of driven quantum systems is: What is the fate of a generic quantum state under repeated application of U_F? In other words, do driven systems thermalize and lose all quantum coherence over time, or can they host stable, non-equilibrium phases of matter with long-lived quantum structure?

In generic interacting Floquet systems, energy is not conserved, and repeated driving typically leads to indefinite heating. According to the *Eigenstate Thermalization Hypothesis* (ETH) [5, 6], such systems are expected to thermalize to an effective infinite-temperature ensemble, where all local information is lost and the system becomes maximally mixed.

However, certain mechanisms can prevent this thermalization. In particular, *many-body localization* (MBL) [4], which results from strong disorder and interaction effects, can inhibit energy absorption and preserve memory of the initial state. When MBL is present, it becomes possible to stabilize rich non-equilibrium phases, including *Floquet symmetry-protected topological* (SPT) [7] phases that are uniquely dynamical and have no equilibrium analogs.

These two extremes: ETH-driven thermalization versus MBL-protected order define fundamentally different dynamical behaviors in Floquet systems. Floquet ETH systems exhibit rapid entanglement growth, decay of local observables, and level statistics consistent with random matrix theory [5, 6]. In contrast, Floquet SPT-MBL systems [8] retain topological edge modes, bounded entanglement entropy, and exhibit coherent oscillations that are robust to disorder and decoherence.

The goal of this article is to provide a comparative theoretical overview of Floquet ETH and Floquet SPT-MBL systems. We explore the underlying mechanisms, key physical observables, and their signatures in both numerical simulations and potential quantum computing implementations. Through this lens, we highlight how these phases provide a window into thermalization, localization, and dynamical topology in driven quantum systems.

2 Floquet Systems and Stroboscopic Dynamics

Floquet systems are characterized by a time-periodic Hamiltonian $H(t)$, satisfying [4]

$$H(t+T) = H(t),$$

for some fixed driving period T. This temporal periodicity allows us to define the system's evolution over discrete time steps rather than continuously, leading to what is called *stroboscopic dynamics* [9].

The evolution operator for one period of the drive, known as the *Floquet operator* or *Floquet unitary*, is given by [1, 4]

$$U_F = \mathcal{T} \exp\left(-i \int_0^T H(t)\, dt\right),$$

where $\mathcal{T}$ denotes time ordering. This operator encodes all information about the system's evolution at stroboscopic times $t = nT$, where $n \in \mathbb{Z}$:

$$|\psi(nT)\rangle = U_F^n |\psi(0)\rangle.$$

The eigenstates $|\phi_\alpha\rangle$ of U_F satisfy

$$U_F|\phi_\alpha\rangle = e^{-i\varepsilon_\alpha T}|\phi_\alpha\rangle,$$

where ε_α are known as *quasienergies*. Due to the periodicity of the exponential function, quasienergies are only defined modulo $2\pi/T$. Consequently, the Floquet spectrum forms a compact Brillouin zone in quasienergy space, analogous to the energy bands in crystals with periodic spatial structure.

This formalism gives rise to an effective description of the dynamics in terms of a time-independent operator, even though the underlying Hamiltonian is time-dependent. In many cases, one introduces a formal *effective Hamiltonian* H_F such that

$$U_F = e^{-iH_F T},$$

although this effective Hamiltonian is often highly non-local and may not admit a simple analytical form.

Understanding the properties of the Floquet operator like its eigenstates, spectrum, and entanglement structure is essential for classifying non-equilibrium phases of matter. Since energy is not conserved, the usual thermodynamic classification based on ground state phases breaks down. Instead, new dynamical phases can emerge, some of which have no equilibrium counterparts.

Depending on the nature of the drive and interactions, a Floquet system may exhibit drastically different behaviors. For example, in thermalizing systems that obey the eigenstate thermalization hypothesis (ETH), the repeated action of U_F leads to heating and loss of coherence. By contrast, in systems with strong disorder and localization (MBL), the dynamics governed by U_F can stabilize novel states such as Floquet time crystals and symmetry-protected topological (SPT) phases.

Importantly, Floquet systems provide an experimentally viable platform for realizing and controlling such exotic phenomena. Because the drive is engineered externally, researchers can tune both the structure of the Hamiltonian and the duration of each step, offering a high degree of flexibility. This has led to a surge of interest in simulating Floquet dynamics using quantum computers [10, 11], trapped ions [12, 13], cold atoms [14, 15], and superconducting qubits [16].

The interplay of drive frequency, interaction strength, disorder, and symmetry thus forms the core of understanding stroboscopic quantum phases. In the sections that follow, we examine two contrasting regimes: thermalizing Floquet ETH systems and non-thermalizing Floquet SPT-MBL systems.

3 Floquet SPT-MBL Systems

In stark contrast to the thermalizing behavior of Floquet ETH systems, certain periodically driven quantum systems can avoid heating and instead support stable, non-thermal dynamical phases of matter. One of the most remarkable examples is the *Floquet symmetry-protected topological* (SPT) [7] phase stabilized by *many-body localization* (MBL) [17]. These phases exhibit robust edge coherence, long-lived dynamical order, and topological features that cannot be realized in equilibrium settings [18].

The existence of Floquet SPT-MBL phases relies on three crucial ingredients. First, the system must possess a discrete global symmetry, such as $\mathbb{Z}_2 \times \mathbb{Z}_2$, which protects the topological nature of the phase. Second, strong disorder must be present to localize bulk degrees of freedom and prevent the absorption of energy from the drive, thereby avoiding thermalization. Third, the time-periodic driving protocol must alternate between symmetry-preserving Hamiltonians that individually may not exhibit topological order but together induce non-trivial Floquet dynamics.

A canonical example of such a system is described by a Floquet unitary operator composed of two steps [18]:

$$U_F = \exp\left(-iJ\sum_j X_{j-1}Z_jX_{j+1}\right)\cdot\exp\left(-i\sum_j h_jZ_j\right),$$

where the first exponential encodes entangling three-site cluster interactions, and the second exponential applies local disordered Z-field rotations. The combination of these steps generates non-trivial dynamics while preserving the required symmetry. This protocol is known to host a Floquet phase that supports edge-localized modes protected by both the disorder-induced localization and the symmetry of the drive.

One of the most striking features of the Floquet SPT-MBL phase is the emergence of quasienergy π-modes localized at the system's boundaries. These edge modes are defined by the property that under one Floquet cycle, the edge-localized operators Γ_L and Γ_R transform as [7, 19, 20]

$$U_F\Gamma_{L,R}U_F^{-1} = -\Gamma_{L,R},$$

implying that the corresponding edge spins exhibit a dynamical flipping with period $2T$, even though the drive itself has period T. This dynamical behavior is a hallmark of Floquet topology and cannot be mimicked by any static Hamiltonian.

The resulting dynamics display a number of experimentally accessible signatures. Edge observables, such as $\langle X_0(t)\rangle$, show persistent oscillations with period $2T$ over long time scales. These oscillations are robust to small perturbations and moderate levels of noise, as long as the protecting symmetry and localization are maintained. In the bulk, the entanglement entropy grows logarithmically with time, a behavior characteristic of MBL systems [21, 22]. This bounded growth enables

the preservation of quantum coherence for edge degrees of freedom, even in the presence of bulk disorder and interactions.

The physical mechanism underlying this phenomenon lies in the interplay between localization and symmetry. The strong disorder localizes the bulk, suppressing resonant interactions and preventing delocalization. Meanwhile, the periodic driving structure and symmetry enforce a coherent, topologically nontrivial evolution of the edge states. Together, these features create a stable dynamical phase with protected edge modes that oscillate in time and do not decohere.

Floquet SPT-MBL systems thus realize a fundamentally new class of quantum phases: they are inherently non-equilibrium and exhibit topological order throughout the spectrum, rather than in just the ground state. They can be realized without the need for cooling or adiabatic preparation, and are particularly well suited for implementation on noisy intermediate-scale quantum (NISQ) devices. The robustness of edge modes to thermalization makes them promising candidates for quantum memory and dynamical quantum error suppression in near-term hardware platforms.

4 Theoretical Comparison and 6-Qubit Simulation Example

From Hamiltonians to gates (short and simple)

Key idea. A Hamiltonian H running for time t makes a unitary gate:

$$U(t) = e^{-iHt}.$$

So "turning on" H for a duration is the same as applying a gate.

If H has many terms: $H = \sum_k H_k$.

- If the H_k *commute*, apply their gates in any order (or in parallel):

$$e^{-i(H_1+\cdots+H_m)t} = \prod_{k=1}^{m} e^{-iH_k t}.$$

- If they *don't* commute, use a short time step Δt (Trotter):

$$e^{-i(H_1+\cdots+H_m)t} \approx \Big(\prod_{k=1}^{m} e^{-iH_k \Delta t}\Big)^{t/\Delta t}.$$

  Smaller $\Delta t \Rightarrow$ smaller error.

Definition of H and S gates The *Hadamard* gate H and the *phase* gate S are standard single-qubit gates:

$$H = \tfrac{1}{\sqrt{2}}\begin{pmatrix} 1 & 1 \\ 1 & -1 \end{pmatrix}, \qquad S = \begin{pmatrix} 1 & 0 \\ 0 & i \end{pmatrix} = R_z\big(\tfrac{\pi}{2}\big), \qquad S^\dagger = \begin{pmatrix} 1 & 0 \\ 0 & -i \end{pmatrix} = R_z\big(-\tfrac{\pi}{2}\big).$$

Intuition. H swaps the Z and X axes (it maps the computational basis to the X basis). S is a 90° rotation around Z.

Useful conjugation rules (for basis changes):

$$HZH = X, \quad HXH = Z, \quad HYH = -Y; \qquad SXS^\dagger = Y, \quad SYS^\dagger = -X, \quad SZS^\dagger = Z.$$

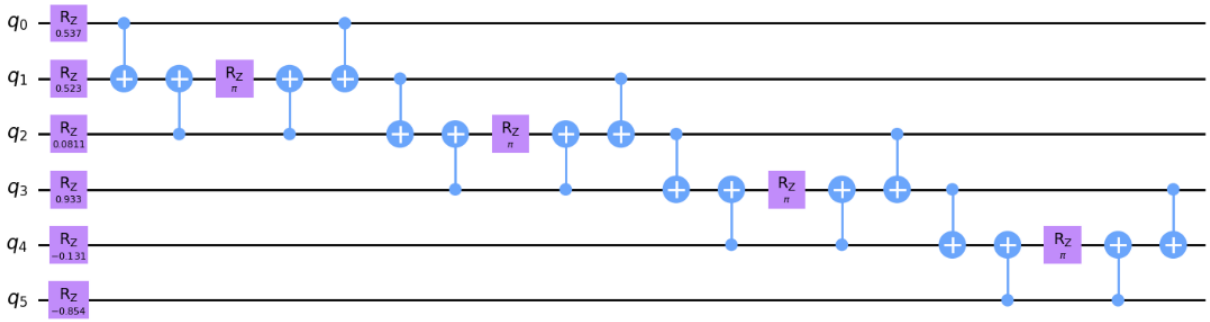

Figure 1: One Floquet period implementing Eq. (3) for N=6: disordered R_z layer followed by compiled XZX cluster terms.

These identities are exactly what we use to turn X or Y factors into Z (and back) when compiling Pauli-string exponentials into circuits.

Trnaslating Pauli terms into quantum circuits: Most model Hamiltonians are sums of Pauli "strings". Each string becomes a small circuit:

- *Single qubit.*

$$e^{-i\theta Z} = R_z(2\theta), \quad e^{-i\theta X} = H\, R_z(2\theta)\, H, \quad e^{-i\theta Y} = S^\dagger H\, R_z(2\theta)\, HS.$$

- *Many qubits.* First rotate each factor to Z (using H or $S^\dagger H$), so the term is $Z \otimes \cdots \otimes Z$. Then:

  1. **Parity trick:** use CNOTs to copy the Z-parity onto one "target" qubit,
  2. apply a single $R_z(2\theta)$ on that target,
  3. uncompute the parity with the same CNOTs,
  4. undo the local rotations.

Two quick examples: [23, 24]

Ising: $e^{-i\theta Z_i Z_j} = \mathrm{CNOT}_{i\to j}\, R_z^{(j)}(2\theta)\, \mathrm{CNOT}_{i\to j}$,

Cluster: $e^{-i\theta X_{j-1} Z_j X_{j+1}} = H_{j-1} H_{j+1}\, \mathrm{CNOT}_{j-1\to j}\, \mathrm{CNOT}_{j+1\to j}\, R_z^{(j)}(2\theta)\, \mathrm{CNOT}_{j+1\to j}\, \mathrm{CNOT}_{j-1\to j}\, H_{j-1} H_{j+1}$.

That's the whole recipe: "exponentiate the Hamiltonian" means turn each term into a small gate block, and combine blocks with Trotter if needed [For more detail please refer to appendix. A].

4.1 Circuit Realization

Each period consists of parallel $R_z(2h_j)$ followed by compiled XZX interactions. We realize $e^{-iJX_{j-1}Z_jX_{j+1}}$ using two Hadamards on the neighbors, a parity-to-target mapping with two CNOTs, a single $R_z(2J)$ on site j, and uncomputation [refer to app.A]; this uses only nearest-neighbor entanglers. A rendered period for N=6 is shown in Fig. 1.

4.2 Observables and Protocol

To expose the edge π-mode, we initialize a product state (here $|+\rangle^{\otimes N}$), then at stroboscopic times $t = nT$ record: (i) edge $\langle X_0\rangle$, (ii) a bulk probe $\langle Z_2\rangle$, and entropies (iii) single-qubit S_0 and (iv) half-chain $S_{\{0,1,2\}}$. We also split $\langle X_0\rangle$ into even/odd periods and compute its FFT.

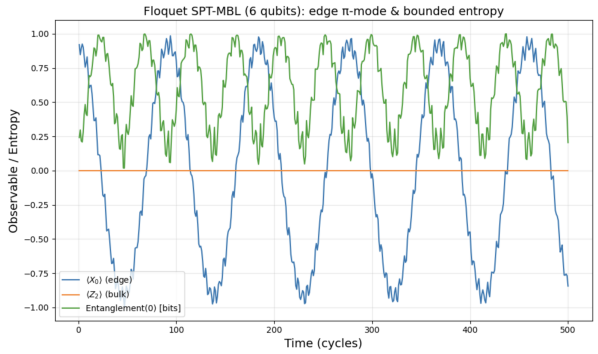

(a) Time series: persistent edge π-mode in $\langle X_0 \rangle$ (blue), small bulk response $\langle Z_2 \rangle$ (orange), and bounded S_0 (green).

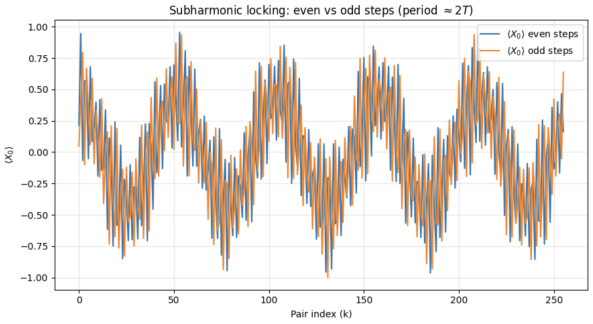

(b) Subharmonic locking of the edge signal: even (blue) and odd (orange) periods share the same envelope with opposite sign (period $\approx 2T$). The slow envelope is a finite-size beat.

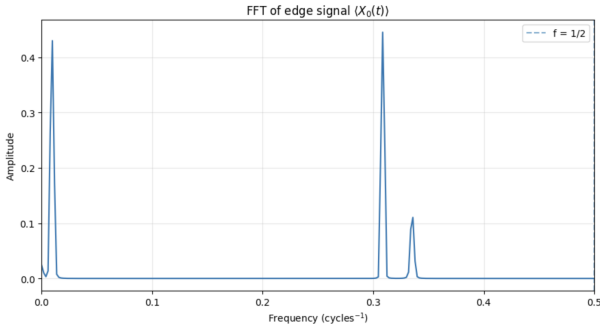

(c) FFT of $\langle X_0(t) \rangle$: dominant peak at $f = \frac{1}{2}$, the smoking-gun of the edge π-mode; small side peaks from weak edge–bulk hybridization/quasienergy splitting.

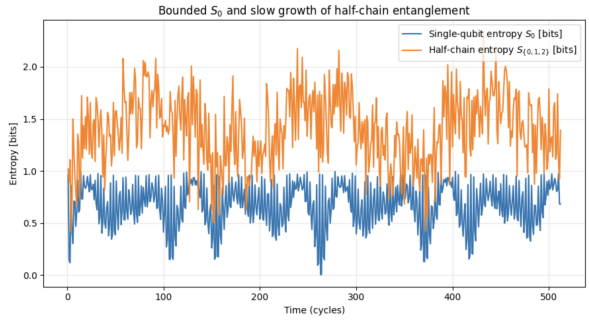

(d) Entanglement diagnostics: S_0 remains bounded (area-law at the edge); $S_{\{0,1,2\}}$ grows slowly and subthermally, consistent with MBL.

Figure 2: Four complementary diagnostics for the SPT–MBL phase under the drive in Eq. (3) (open chain, N=6). Together they indicate a protected edge π-mode stabilized by disorder and $\mathbb{Z}_2 \times \mathbb{Z}_2$ symmetry.

5 Interpretation of Simulation Results: MBL–SPT Diagnostics

This section interprets the updated 6-qubit Floquet simulations with $\mathbb{Z}_2 \times \mathbb{Z}_2$ symmetry. The combined evidence is consistent with a many-body localized (MBL) symmetry-protected topological (SPT) phase stabilized by disorder and the protecting symmetry.

Interpretation of Fig. 2a (time–series diagnostics)

Figure 2a shows the stroboscopic dynamics for three readouts on a N=6 open chain: the edge observable $\langle X_0 \rangle$ (blue), a bulk probe $\langle Z_2 \rangle$ (orange), and the single–qubit entropy $S_0(t)$ (green).

- **Edge π–mode (blue).** The edge signal flips sign from cycle to cycle, producing a clear period–doubled waveform (effective period $\approx 2T$) with $\mathcal{O}(1)$ amplitude maintained over hundreds of periods. A slow envelope modulation is visible and is consistent with finite–size edge–edge hybridization or a small quasienergy splitting from exactly π/T.

- **Localized bulk (orange).** The bulk probe remains pinned near zero with only small fluctuations and no coherent long–period structure, indicating that the driven bulk is localized and weakly coupled to the edge degree of freedom.
- **Bounded entanglement (green).** The single–qubit entropy $S_0(t)$ stays bounded (well below 1 bit) with mild oscillations and no secular growth, consistent with area–law behavior and the absence of drive–induced heating.

Taken together, the coexistence of a robust $2T$ edge oscillation, a quiet bulk signal, and bounded S_0 is the expected time–domain signature of an MBL–protected Floquet SPT regime in this small chain. (Even/odd locking and the $f = \frac{1}{2}$ line in the FFT, shown in the other panels, provide complementary confirmation.)

Subharmonic locking in the edge observable. As shown in Fig. 2b, the edge signal $\langle X_0 \rangle$ split into even and odd periods exhibits the same envelope with opposite sign, indicating a period-doubled (subharmonic) response with period $\approx 2T$. This is the time-domain signature of a Floquet π-mode localized at the boundary. The persistence of the alternation over many cycles indicates coherence protection provided by MBL.

Frequency-space signature. The Fourier spectrum of $\langle X_0(t) \rangle$ contains a sharp line at $f = \frac{1}{2}$ (in cycles^{-1}), see Fig. 2c, which is the frequency-space counterpart of the $2T$ subharmonic oscillation. The narrow peak reflects a stable oscillation frequency. Small side peaks are attributable to finite-size effects and weak edge–bulk coupling.

Entanglement dynamics. Figure 2d shows that the single-qubit entropy $S_0(t)$ remains bounded (well below 1 bit), and the half-chain entropy $S_{\{0,1,2\}}(t)$ grows slowly and saturates far below the infinite-temperature value. This is consistent with area-law entanglement and the absence of rapid thermalization in the MBL regime. The mild oscillations in both entropies reflect coherent edge–bulk interplay.

Physical interpretation. Taken together, these diagnostics support the identification of the observed phase as: (i) a Floquet SPT with a robust edge π-mode; (ii) MBL-protected, preventing drive-induced heating and preserving the edge dynamics; and (iii) symmetry-protected under $\mathbb{Z}_2 \times \mathbb{Z}_2$, which forbids symmetric local terms from gapping out the edge degree of freedom.

Conclusion. The observed features persistent subharmonic edge oscillations, a clean $f = \frac{1}{2}$ Fourier peak, and bounded entanglement growth are jointly consistent with an MBL-protected Floquet SPT phase in this small-chain simulation.

6 Floquet SPT-MBL Physics and NISQ Devices

Floquet SPT-MBL phases are exceptionally well-suited to exploration on Noisy Intermediate-Scale Quantum (NISQ) devices. These systems are intrinsically non-equilibrium, requiring only shallow circuits per cycle, which fits naturally within the coherence time constraints of NISQ platforms. The presence of many-body localization ensures robustness to noise and suppression of heating, allowing coherent dynamical signatures (such as π-mode edge oscillations) to persist despite imperfections.

Moreover, the binary drive structure used to realize Floquet SPT-MBL phases, such as alternating disordered Z-rotations and entangling XZX gates, is straightforward to implement using standard native gates on current hardware. Because entanglement growth in the MBL phase is slow and area-law [25], state evolution and measurement remain feasible on modest qubit counts. This makes such models ideal candidates for demonstrating non-trivial quantum dynamics and edge coherence in early quantum processors, thereby serving as testbeds for dynamical topology and quantum memory.

7 Conclusion

Using a minimal N=6 open chain driven by the two–step unitary, we observed the canonical triad of diagnostics for a Floquet SPT–MBL phase: (i) a long-lived, period-doubled edge signal in $\langle X_0 \rangle$ (Fig. 2a,b), (ii) a sharp Fourier line at $f = \frac{1}{2}$ (Fig. 2c), and (iii) bounded single-qubit entropy with slow half-chain growth (Fig. 2d). Together these results indicate a robust edge π-mode stabilized by $\mathbb{Z}_2 \times \mathbb{Z}_2$ symmetry and many-body localization, realized with a shallow circuit compiled from native gates. Finite-size beats and small side peaks are consistent with weak edge–bulk hybridization in a short chain and do not obscure the primary signatures.

Outlook. The same framework naturally extends to (a) disorder averaging and explicit control tests (symmetry breaking, reduced disorder) to sharpen phase boundaries, (b) larger system sizes and hardware noise studies to quantify edge-mode lifetimes, and (c) alternative readouts (randomized purity/entanglement probes) to reduce tomography overhead. These steps turn the present 6-qubit demonstration into a scalable benchmark for dynamical topology and boundary-qubit coherence on near-term devices.

References

[1] J. H. Shirley, "Solution of the schrödinger equation with a hamiltonian periodic in time," *Phys. Rev.*, vol. 138, pp. B979–B987, May 1965.

[2] T. Kitagawa, E. Berg, M. Rudner, and E. Demler, "Topological characterization of periodically driven quantum systems," *Phys. Rev. B*, vol. 82, p. 235114, Dec 2010.

[3] L. D'Alessio and M. Rigol, "Long-time behavior of isolated periodically driven interacting lattice systems," *Phys. Rev. X*, vol. 4, p. 041048, Dec 2014.

[4] P. Ponte, Z. Papić, F. m. c. Huveneers, and D. A. Abanin, "Many-body localization in periodically driven systems," *Phys. Rev. Lett.*, vol. 114, p. 140401, Apr 2015.

[5] J. M. Deutsch, "Quantum statistical mechanics in a closed system," *Phys. Rev. A*, vol. 43, pp. 2046–2049, Feb 1991.

[6] M. Srednicki, "Chaos and quantum thermalization," *Phys. Rev. E*, vol. 50, pp. 888–901, Aug 1994.

[7] A. C. Potter, T. Morimoto, and A. Vishwanath, "Classification of interacting topological floquet phases in one dimension," *Phys. Rev. X*, vol. 6, p. 041001, Oct 2016.

[8] I.-D. Potirniche, A. C. Potter, M. Schleier-Smith, A. Vishwanath, and N. Y. Yao, "Floquet symmetry-protected topological phases in cold-atom systems," *Phys. Rev. Lett.*, vol. 119, p. 123601, Sep 2017.

[9] T. Iadecola, L. H. Santos, and C. Chamon, "Stroboscopic symmetry-protected topological phases," *Phys. Rev. B*, vol. 92, p. 125107, Sep 2015.

[10] T. Oka and S. Kitamura, "Floquet engineering of quantum materials," *Annual Review of Condensed Matter Physics*, vol. 10, no. 1, pp. 387–408, 2019.

[11] A. Eckardt, "Atomic quantum gases in periodically driven optical lattices," *arXiv preprint arXiv:1606.08041*, 2016.

[12] J. W. Britton, B. C. Sawyer, A. C. Keith, C.-C. J. Wang, J. K. Freericks, H. Uys, M. J. Biercuk, and J. J. Bollinger, "Engineered two-dimensional ising interactions in a trapped-ion quantum simulator with hundreds of spins," *Nature*, vol. 484, no. 7395, pp. 489–492, 2012.

[13] P. Hess, J. Zhang, A. Kyprianidis, P. Becker, A. Lee, J. Smith, G. Pagano, I.-D. Potirniche, A. Potter, A. Vishwanath, *et al.*, "Observation of a discrete time crystal," 2017.

[14] M. Lohse, C. Schweizer, O. Zilberberg, M. Aidelsburger, and I. Bloch, "A thouless quantum pump with ultracold bosonic atoms in an optical superlattice," *Nature Physics*, vol. 12, no. 4, pp. 350–354, 2016.

[15] G. Jotzu, M. Messer, R. Desbuquois, M. Lebrat, T. Uehlinger, D. Greif, and T. Esslinger, "Experimental realization of the topological haldane model with ultracold fermions," *Nature*, vol. 515, no. 7526, pp. 237–240, 2014.

[16] P. Roushan, C. Neill, J. Tangpanitanon, V. M. Bastidas, A. Megrant, R. Barends, Y. Chen, Z. Chen, B. Chiaro, A. Dunsworth, *et al.*, "Spectroscopic signatures of localization with interacting photons in superconducting qubits," *Science*, vol. 358, no. 6367, pp. 1175–1179, 2017.

[17] A. Chandran, V. Khemani, C. R. Laumann, and S. L. Sondhi, "Many-body localization and symmetry-protected topological order," *Phys. Rev. B*, vol. 89, p. 144201, Apr 2014.

[18] J. Kemp, N. Y. Yao, and C. R. Laumann, "Symmetry-enhanced boundary qubits at infinite temperature," *Phys. Rev. Lett.*, vol. 125, p. 200506, Nov 2020.

[19] V. Khemani, A. Lazarides, R. Moessner, and S. L. Sondhi, "Phase structure of driven quantum systems," *Phys. Rev. Lett.*, vol. 116, p. 250401, Jun 2016.

[20] D. V. Else and C. Nayak, "Classification of topological phases in periodically driven interacting systems," *Phys. Rev. B*, vol. 93, p. 201103, May 2016.

[21] J. H. Bardarson, F. Pollmann, and J. E. Moore, "Unbounded growth of entanglement in models of many-body localization," *Phys. Rev. Lett.*, vol. 109, p. 017202, Jul 2012.

[22] M. Serbyn, Z. Papić, and D. A. Abanin, "Universal slow growth of entanglement in interacting strongly disordered systems," *Phys. Rev. Lett.*, vol. 110, p. 260601, Jun 2013.

[23] J. D. Whitfield, J. Biamonte, and A. Aspuru-Guzik, "Simulation of electronic structure hamiltonians using quantum computers," *Molecular Physics*, vol. 109, no. 5, pp. 735–750, 2011.

[24] R. Loredo, *Learn quantum computing with Python and IBM quantum experience*. Packt Publishing, 2020.

[25] J. Eisert, M. Cramer, and M. B. Plenio, "Colloquium: Area laws for the entanglement entropy," *Rev. Mod. Phys.*, vol. 82, pp. 277–306, Feb 2010.

A Circuit Construction from Hamiltonian

A.1 Why a Hamiltonian becomes a circuit (the map to remember)

1) Physics law ⇒ gate. Quantum time evolution is unitary and generated by the Hamiltonian:

$$i\,\frac{d}{dt}\psi(t) = H\psi(t) \quad \Longrightarrow \quad \psi(t) = U(t)\psi(0), \qquad U(t) = e^{-iHt}.$$

So "turning on" H for time t *is* a gate $U(t)$. Digital simulation means we factor $U(t)$ into native one- and two-qubit gates.

2) One Pauli string ⇒ one small block. Most model Hamiltonians are sums of Pauli strings. If P is a k-qubit Pauli string ($P^2 = \mathbb{1}$, eigenvalues ± 1), then

$$e^{-i\theta P} = \cos\theta\,\mathbb{1} - i\sin\theta\,P.$$

Implementing $e^{-i\theta P}$ is easy once P is turned into a single Z on some *parity qubit*. Formally, find a unitary V such that

$$V\,P\,V^\dagger = Z_{\text{parity}}, \quad \Rightarrow \quad e^{-i\theta P} = V^\dagger\, e^{-i\theta Z_{\text{parity}}}\, V = V^\dagger\, R_z(2\theta)_{\text{parity}}\, V.$$

The circuit is thus: *(basis changes) → compute parity → $R_z(2\theta)$ → uncompute parity → undo basis changes.*

3) Basis changes for $X, Y \to Z$. Local single-qubit identities:

$$e^{-i\theta Z} = R_z(2\theta), \qquad e^{-i\theta X} = H\,R_z(2\theta)\,H, \qquad e^{-i\theta Y} = S^\dagger H\,R_z(2\theta)\,HS,$$

because $HZH = X$ and $SXS^\dagger = Y$. *Rule:* rotate each non-Z factor to Z, do the work in Z basis, rotate back.

4) Why the "parity trick" works (CNOT conjugation). CNOT copies Z *parity* from control to target under conjugation:

$$\text{CNOT}^\dagger_{a\to b}\, Z_b\, \text{CNOT}_{a\to b} = Z_a Z_b, \qquad \text{CNOT}^\dagger_{a\to b}\, Z_a\, \text{CNOT}_{a\to b} = Z_a.$$

Hence two CNOTs onto a middle qubit j map $Z_j \mapsto Z_{j-1}Z_jZ_{j+1}$:

$$\text{CNOT}_{j-1\to j}\ \text{CNOT}_{j+1\to j}\ Z_j\ \text{CNOT}_{j+1\to j}\ \text{CNOT}_{j-1\to j} = Z_{j-1}Z_jZ_{j+1}.$$

Exponentiating preserves the identity, so

$$e^{-i\theta Z_{j-1}Z_jZ_{j+1}} = \text{CNOT}_{j-1\to j}\,\text{CNOT}_{j+1\to j}\ e^{-i\theta Z_j}\ \text{CNOT}_{j+1\to j}\,\text{CNOT}_{j-1\to j}.$$

Combine with the basis changes above to get XZX (our cluster term).

5) Two canonical examples (commit to memory).

$$\boxed{e^{-i\theta Z_iZ_j} = \text{CNOT}_{i\to j}\ R_z^{(j)}(2\theta)\ \text{CNOT}_{i\to j}}$$

$$\boxed{e^{-i\theta X_{j-1}Z_jX_{j+1}} = H_{j-1}H_{j+1}\ \text{CNOT}_{j-1\to j}\,\text{CNOT}_{j+1\to j}\ R_z^{(j)}(2\theta)\ \text{CNOT}_{j+1\to j}\,\text{CNOT}_{j-1\to j}\ H_{j-1}H_{j+1}}$$

6) Sums of terms ⇒ Trotter product. If $H = \sum_k H_k$, commuting pieces can be done in any order (or in parallel): $e^{-i(\sum_k H_k)t} = \prod_k e^{-iH_k t}$. If not, use short steps Δt (Lie–Trotter/Suzuki):

$$e^{-i(H_1+H_2)t} \approx \left(e^{-iH_1\,\Delta t}\, e^{-iH_2\,\Delta t}\right)^{t/\Delta t} \quad \text{(1st order; error } \mathcal{O}(\Delta t)\text{)}.$$

A popular symmetric 2nd order cancels the leading error:

$$e^{-i(H_1+H_2)t} \approx \left(e^{-iH_1\,\Delta t/2}\, e^{-iH_2\,\Delta t}\, e^{-iH_1\,\Delta t/2}\right)^{t/\Delta t}.$$

7) Mental checklist (never forget).

1. **Law:** gates are e^{-iHt}.
2. **Per term:** rotate $X/Y \to Z$ locally.
3. **Parity:** CNOTs compute Z-parity onto one target.
4. **Phase:** do a single $R_z(2\theta)$ on that target.
5. **Uncompute & undo** to restore the register.
6. **Sum of terms:** Trotter when they do not commute; parallelize when they do.

This is the rationale behind turning any Pauli-string Hamiltonian into a short gate block. Your Floquet SPT drive uses exactly this recipe: the disorder layer is parallel R_z gates, and the cluster layer is a three-body Pauli string compiled via basis changes + parity + one R_z.

B Appendix: Simulation Code Listings

A.1 Floquet SPT-MBL Circuit Construction (Qiskit)

```
import numpy as np
from qiskit import QuantumCircuit
from qiskit.visualization import plot_circuit_layout

def floquet_spt_step(n_qubits, h_fields, J):
    """
    Build a Qiskit QuantumCircuit that implements one Floquet step
    for the Floquet SPT-MBL model with:
    - disordered Z-fields (localization),
    - three-body XZX interactions (SPT entanglers).

    U_F = U_2 · U_1, where:
        U_1 = exp(-i  h_j Z_j)    -- local field disorder
        U_2 = exp(-i J  X_{j-1} Z_j X_{j+1}) -- entanglers

    Parameters:
        n_qubits : int
            Number of qubits in the chain (must be  3)
        h_fields : array_like
```

```
            Random disorder values h_j for each qubit
        J : float
            Coupling strength for the XZX cluster terms

    Returns:
        QuantumCircuit
            Qiskit circuit implementing the Floquet step
    """
    qc = QuantumCircuit(n_qubits)

    # Step 1: Apply local disordered Z-rotations (U_1)
    for j in range(n_qubits):
        qc.rz(2 * h_fields[j], j)

    # Step 2: Apply compiled XZX three-body interactions (U_2)
    for j in range(1, n_qubits - 1):
        qc.cx(j - 1, j)            # first half of XZX
        qc.cx(j + 1, j)
        qc.rz(2 * J, j)            # conditional Z-rotation on middle qubit
        qc.cx(j + 1, j)            # undo
        qc.cx(j - 1, j)

    return qc

# ----------------------------
# Example: Generate and visualize a 6-qubit circuit
# ----------------------------
n = 6
J = np.pi / 2                              # Interaction strength
h_random = np.random.uniform(-0.5, 0.5, n)  # Disorder realization

# Construct one Floquet unitary step
qc_step = floquet_spt_step(n_qubits=n, h_fields=h_random, J=J)

# Draw the circuit
qc_step.draw("mpl")  # Use "mpl" for graphical rendering in Jupyter
```

Floquet SPT–MBL on a 6-Qubit Chain

```
import numpy as np
import matplotlib.pyplot as plt
from qiskit import QuantumCircuit
from qiskit.quantum_info import Statevector, SparsePauliOp, partial_trace
# ----------------------------------
# Helpers
# ----------------------------------
```

```
def pauli_on(n, q, char):  # char in {"X","Y","Z"}
    # Qiskit uses little-endian labels: rightmost char is qubit 0.
    lbl = ["I"] * n
    lbl[n - 1 - q] = char
    return SparsePauliOp.from_list([("".join(lbl), 1.0)])

def single_qubit_entropy(rhoA):
    # rhoA is a 2x2 DensityMatrix (qiskit object with .data)
    evals = np.linalg.eigvalsh(rhoA.data)
    evals = np.clip(evals.real, 1e-12, 1.0)
    return -np.sum(evals * np.log2(evals))

# ------------------------------------
# One Floquet SPT-MBL step
# U_F = exp(-i * sum_j h_j Z_j) · exp(-i * J * sum_j X_{j-1} Z_j X_{j+1})
# ------------------------------------
def floquet_spt_step(n, h_fields, J):
    qc = QuantumCircuit(n)
    # Step 1: disordered on-site Z rotations
    for j in range(n):
        qc.rz(2 * h_fields[j], j)      # e^{-i h Z} = Rz(2h)
    # Step 2: cluster XZX terms (open chain -> j = 1..n-2)
    for j in range(1, n - 1):
        # Conjugate ZZZ with H on neighbors to get XZX
        qc.h(j - 1); qc.h(j + 1)
        # Compute parity of neighbors onto qubit j, rotate, uncompute
        qc.cx(j - 1, j); qc.cx(j + 1, j)
        qc.rz(2 * J, j)
        qc.cx(j + 1, j); qc.cx(j - 1, j)
        qc.h(j - 1); qc.h(j + 1)
    return qc

# ----------------------------
# Parameters
# ----------------------------
n = 6
J = np.pi / 4          # /4{/2 both used; /4 is gentle
steps = 500
W = 0.8                # disorder width
np.random.seed(42)
h_fields = np.random.uniform(-W, W, n)

# ----------------------------
# Initial state: edge in |+>, bulk in |+>
# (Use |+> on edge to see period-doubled ⟨X0⟩ oscillations.)
# ----------------------------
init = QuantumCircuit(n)
init.h(range(n))            # |+>^n
```

```
psi = Statevector.from_instruction(init)

# ----------------------------
# Observables
# ----------------------------
X0 = pauli_on(n, 0, "X")
Z0 = pauli_on(n, 0, "Z")
Z2 = pauli_on(n, 2, "Z")

times, x0s, z0s, z2s, S0 = [], [], [], [], []

# ----------------------------
# Floquet evolution
# ----------------------------
for t in range(1, steps + 1):
    psi = psi.evolve(floquet_spt_step(n, h_fields, J))

    # Edge and bulk observables
    x0s.append(np.real(psi.expectation_value(X0)))
    z0s.append(np.real(psi.expectation_value(Z0)))
    z2s.append(np.real(psi.expectation_value(Z2)))

    # Single-qubit (qubit 0) entanglement entropy, in bits
    rho0 = partial_trace(psi, list(range(1, n)))  # trace out 1..n-1
    S0.append(single_qubit_entropy(rho0))

    times.append(t)

# ----------------------------
# Plot
# ----------------------------
plt.figure(figsize=(10, 6))
plt.plot(times, x0s, label=r'$\langle X_0\rangle$ (edge)')
plt.plot(times, z2s, label=r'$\langle Z_2\rangle$ (bulk)')
plt.plot(times, S0,  label='Entanglement(0) [bits]')
plt.xlabel("Time (cycles)", fontsize=14)
plt.ylabel("Observable / Entropy", fontsize=14)
plt.title("Floquet SPT-MBL (6 qubits): edge -mode & bounded entropy", fontsize=14)
plt.legend()
plt.grid(alpha=0.3)
plt.tight_layout()
plt.show()
```

A.3 Floquet ETH Model Code: (1) Subharmonic (period-doubled) edge dynamics (2) FFT of the edge signal (3) Bounded single-qubit entropy S0(t) and slow half-chain entanglement growth

```
# PURPOSE
# -------
# Simulate a 6-qubit 1D Floquet SPT-MBL circuit and visualize three key diagnostics:
#   (1) Subharmonic (period-doubled) edge dynamics via <X0> at even vs odd steps
#   (2) FFT of the edge signal showing a peak at f = 1/2 (the -mode)
#   (3) Bounded single-qubit entropy S0(t) and slow half-chain entanglement growth
#
# Model (open chain):
#   U_F = exp[-i * sum_j h_j Z_j]  ·  exp[-i * J * sum_j X_{j-1} Z_j X_{j+1}]
# Implementation notes:
#   • The XZX cluster term is compiled using H on the neighbors + 4 CNOTs + Rz + uncompute.
#   • Qiskit uses little-endian Pauli labels: rightmost character is qubit 0.
#   • J  /2 produces a clean -mode (exact edge toggle per period).
#
# Try changing:
#   • J:  np.pi/2 (sharp -mode), np.pi/4 (softer/quasiperiodic)
#   • W:  disorder width (e.g., 0.8{1.2) | enough to localize and avoid heating
#   • init: edge in |+> (init.h(0)) vs |+>^{n} for different visibility
# ------------------------------------------------------------------------------

import numpy as np
import matplotlib.pyplot as plt
from qiskit import QuantumCircuit
from qiskit.quantum_info import Statevector, SparsePauliOp, partial_trace

# ---------- utilities ----------
def pauli_on(n, q, char):
    """Return a SparsePauliOp for a single-qubit Pauli on qubit q (0 = leftmost).
    Qiskit label order is little-endian: rightmost character is qubit 0."""
    lbl = ["I"] * n
    lbl[n - 1 - q] = char  # place Pauli at the correct (little-endian) position
    return SparsePauliOp.from_list([("".join(lbl), 1.0)])

def von_neumann_entropy(dm):
    """Von Neumann entropy S() in bits for a qiskit DensityMatrix-like object."""
    eig = np.linalg.eigvalsh(dm.data).real
    eig = np.clip(eig, 1e-12, 1.0)  # numerical safety
    return -np.sum(eig * np.log2(eig))

# ---------- one Floquet step:   U_F = e^{-i  h_j Z_j} · e^{-i J  X_{j-1} Z_j X_{j+1}} -------
def floquet_spt_step(n, h_fields, J):
    qc = QuantumCircuit(n)

    # (1) Disordered on-site Z rotations: e^{-i h_j Z_j} = Rz(2 h_j)
```

```
    for j in range(n):
        qc.rz(2 * h_fields[j], j)

    # (2) Cluster XZX interactions on sites j-1, j, j+1 (open chain: j = 1..n-2)
    #     e^{-i J X_{j-1} Z_j X_{j+1}}
    #   = (H_{j-1}  I_j  H_{j+1})
    #     · [CNOT_{j-1→j} CNOT_{j+1→j} Rz_j(2J) CNOT_{j+1→j} CNOT_{j-1→j}]
    #     · (H_{j-1}  I_j  H_{j+1})
    for j in range(1, n - 1):
        qc.h(j - 1); qc.h(j + 1)
        qc.cx(j - 1, j); qc.cx(j + 1, j)
        qc.rz(2 * J, j)
        qc.cx(j + 1, j); qc.cx(j - 1, j)
        qc.h(j - 1); qc.h(j + 1)

    return qc

# ---------- parameters ----------
n = 6
steps = 512                 # power of 2 → cleaner FFT
J = np.pi / 4               # exact -mode (toggle each period)
W = 0.8                     # disorder width; ~0.8{1.2 works well
np.random.seed(7)
h_fields = np.random.uniform(-W, W, n)

# ---------- initial state ----------
# Edge -mode is most visible with the edge in |+>. Here we set |+>^{n}.
# For an even starker edge signal, try: init = QuantumCircuit(n); init.h(0)
init = QuantumCircuit(n)
init.h(range(n))
psi = Statevector.from_instruction(init)

# ---------- observables ----------
X0 = pauli_on(n, 0, "X")    # edge X (-mode lives here)
Z2 = pauli_on(n, 2, "Z")    # a bulk Z probe

# storage for time series
tlist, x0, z2, S0, S_half = [], [], [], [], []

# ---------- evolve for 'steps' Floquet periods ----------
for t in range(1, steps + 1):
    psi = psi.evolve(floquet_spt_step(n, h_fields, J))

    # edge/bulk expectation values
    x0.append(np.real(psi.expectation_value(X0)))
    z2.append(np.real(psi.expectation_value(Z2)))

    # single-qubit entropy (qubit 0) | should stay bounded (< 1 bit)
```

```
    rho0 = partial_trace(psi, list(range(1, n)))  # keep {0}
    S0.append(von_neumann_entropy(rho0))

    # half-chain entropy for A = {0,1,2} | slow growth in MBL
    rhoA = partial_trace(psi, [3, 4, 5])         # trace out complement → keep {0,1,2}
    S_half.append(von_neumann_entropy(rhoA))

    tlist.append(t)

# ---------- (i) even vs odd steps: subharmonic locking (period ~ 2T) ----------
x_even = x0[0::2]
x_odd  = x0[1::2]
k = np.arange(len(x_even))  # cycle pairs

plt.figure(figsize=(9, 5))
plt.plot(k, x_even, label=r'$\langle X_0\rangle$ even steps')
plt.plot(k, x_odd,  label=r'$\langle X_0\rangle$ odd steps')
plt.xlabel('Pair index (k)'); plt.ylabel(r'$\langle X_0\rangle$')
plt.title(r'Subharmonic locking: even vs odd steps (period $\approx 2T$)')
plt.legend(); plt.grid(alpha=0.3); plt.tight_layout()
plt.show()

# ---------- (ii) FFT of <X0>: dominant peak at f = 1/2 ----------
x0_centered = np.array(x0) - np.mean(x0)       # remove DC
w = np.hanning(len(x0_centered))               # window to reduce leakage
xw = x0_centered * w

freqs = np.fft.rfftfreq(len(xw), d=1.0)        # units: cycles^{-1}
amp   = np.abs(np.fft.rfft(xw)) * 2.0 / np.sum(w)  # single-sided, roughly normalized

plt.figure(figsize=(9, 5))
plt.plot(freqs, amp)
plt.axvline(0.5, ls='--', alpha=0.6, label='f = 1/2')
plt.xlim(0, min(0.52, freqs.max()))
plt.xlabel(r'Frequency (cycles$^{-1}$)')
plt.ylabel('Amplitude')
plt.title(r'FFT of edge signal $\langle X_0(t)\rangle$')
plt.legend()
plt.grid(alpha=0.3); plt.tight_layout(); plt.show()

# ---------- (iii) entanglement diagnostics ----------
plt.figure(figsize=(9, 5))
plt.plot(tlist, S0,     label=r'Single-qubit entropy $S_0$ [bits]')
plt.plot(tlist, S_half, label=r'Half-chain entropy $S_{\{0,1,2\}}$ [bits]')
plt.xlabel('Time (cycles)'); plt.ylabel('Entropy [bits]')
plt.title(r'Bounded $S_0$ and slow growth of half-chain entanglement')
plt.legend()
plt.grid(alpha=0.3); plt.tight_layout(); plt.show()
```